

Predictive eye movements are adjusted in a Bayes-optimal fashion in response to unexpectedly changing environmental probabilities

Arthur, T. & Harris, D.J.

Abstract

This study examined the application of active inference to dynamic visuomotor control. Active inference proposes that actions are dynamically planned according to uncertainty about sensory information, prior expectations, and the environment, with motor adjustments serving to minimise future prediction errors. We investigated whether predictive gaze behaviours are indeed adjusted in this Bayes-optimal fashion during a virtual racquetball task. In this task, participants intercepted bouncing balls with varying levels of elasticity, under conditions of higher or lower environmental volatility. Participants' gaze patterns differed between stable and volatile conditions in a manner consistent with generative models of Bayes-optimal behaviour. Partially observable Markov models also revealed an increased rate of associative learning in response to unpredictable shifts in environmental probabilities, although there was no overall effect of volatility on this parameter. Findings extend active inference frameworks into complex and unconstrained visuomotor tasks and present important implications for a neurocomputational understanding of the visual guidance of action.

Keywords: active inference; Bayesian; predictive coding; visuomotor; virtual reality

Predictive eye movements are adjusted in a Bayes-optimal fashion in response to unexpectedly changing environmental probabilities

1. Introduction

1 The visual guidance of movement involves strategic gaze shifts towards spatial locations that
2 inform future actions (de Brouwer et al., 2021; Land, 2009; Zhao & Warren, 2015). Gaze shifts are
3 partly driven by mental models of the scene and expectations about the location of important
4 information (Henderson, 2017; Itti & Koch, 2001), but inherent processing delays can limit our ability
5 to monitor dynamic and unstable visual cues. To combat these systemic shortfalls, gaze is controlled
6 in an anticipatory manner, based on estimations of the current state and learned properties of the
7 environment (Diaz, Cooper, & Hayhoe, 2013; Hayhoe et al., 2012; Mrotek & Soechting, 2007;
8 Nijhawan, 2008). For instance, when hitting a ball, agents generally execute a saccade to its
9 *predicted* future location, situating their fixation a few degrees above likely bounce positions (Mann
10 et al., 2019). While these anticipatory gaze strategies seem to be pervasive (Diaz, Cooper, & Hayhoe,
11 2013; Diaz, Cooper, Rothkopf, et al., 2013), it is less clear how they are adjusted when an agent
12 becomes uncertain about their predictions. Picture, for instance, a tennis player trying to return a
13 ball on a rough surface, or a batsman in cricket attempting to play a ball delivered with unknown
14 direction and degree of spin. Is the optimal strategy to stop predicting and rely on online
15 information, or to modify predictions in line with the additional uncertainty and persist with
16 anticipatory eye movements?

17 Bayesian theories of perception propose that the brain responds to uncertainty by adjusting
18 predictions in a statistically optimal fashion (Knill & Pouget, 2004; Körding & Wolpert, 2004; Rao &
19 Ballard, 1999). Beliefs about hidden states – such as the origin of sensory information or the likely
20 behaviour of the tennis ball – are believed to be the result of integrating top-down expectations
21 with bottom-up sensations (Knill & Pouget, 2004; Körding, 2007; Körding & Wolpert, 2004; Rauss &
22 Pourtois, 2013). The influence of these informational sources is thought to be scaled according to
23 their *precision* (i.e., inverse of the variance) such that bottom-up sensory signals will have a greater
24 impact on posterior beliefs when predictions are weak (Friston, 2005; Shipp et al., 2013). So, when
25 the tennis court is rough (i.e., predictions are uncertain), the player should rely less heavily on their
26 prior expectations about post-bounce trajectory and place added weight on incoming ball motion
27 information.

28 These Bayes-optimal computations are not only proposed to shape perception (as described
29 by predictive coding; Rao & Ballard, 1999), but also learning and action policy selection (Friston et
30 al., 2016; Parr & Friston, 2019). For both perception and action, agents are said to encode an

31 internal 'generative' model of the world, which simulates expected sensory data and infers the likely
32 causes of sensations to minimise prediction errors, or *variational free-energy* (VFE; Friston et al.,
33 2006; Friston, 2010; Rao & Ballard, 1999). Active inference extends free energy minimisation to the
34 case of actions, where agents seek to select motor plans (or policies) that minimise future free
35 energy, or *expected free energy* (EFE; Parr & Friston, 2019). EFE represents not only the minimisation
36 of prediction error (i.e., information gain), but also the preference for particular outcomes
37 associated with that action.

38 In addition to minimising uncertainty via overt motor actions, fixations and saccades can also
39 be conceptualised as individual hypotheses about the state of the world that are aimed at
40 minimising future prediction errors (also known as Bayesian surprise/surprisal; Friston et al., 2012;
41 Itti & Baldi, 2009; Najemnik & Geisler, 2005). Under these assumptions of free energy minimisation,
42 agents should actively 'sample' the world in a way that minimises EFE. While most empirical support
43 for this notion comes from relatively simple perceptual and motor tasks, a small number of previous
44 investigations have identified the importance of predictive cues in the execution of more
45 unconstrained visuomotor skills (Abernethy et al., 2001; Gray & Cañal-Bruland, 2018; Gredin et al.,
46 2018; Stevenson et al., 2009). These studies have suggested that unreliable prior information may be
47 weighted less heavily by agents when executing a motor response (e.g., during interceptive baseball
48 swings; Gray & Cañal-Bruland, 2018). Nevertheless, such processes have not been explicitly
49 modelled as active inference and the above studies have not considered situations in which
50 environmental statistics change dynamically over time. While a tennis player might know that
51 roughly 5% of balls will behave erratically, this degree of uncertainty could also fluctuate as, for
52 instance, the court gets worn or the balls get older.

53 In fact, previous work has discussed three main types of environmental uncertainty that can
54 affect perception and action (Bland & Schaefer, 2012; Hein et al., 2021; Yu & Dayan, 2005). *Expected*
55 *uncertainty* refers to the inherent ambiguity derived from probabilistic relationships that exist in the
56 world, such as the outcome of a coin toss. *Estimation uncertainty* emerges from imperfect
57 knowledge of those relationships and diminishes as a result of learning (e.g., repeatedly observing
58 that a coin toss is unbiased). *Unexpected uncertainty* or *volatility* refers to changes in expected
59 uncertainty over time, such as a shift in the probabilistic association between a stimulus and an
60 outcome. Bland and Schaefer (2012) further distinguish between these latter constructs, in the
61 sense that unexpected uncertainty is characterised by rare unforeseen changes in probabilistic
62 relationships, while volatility typifies frequent variations that can, in effect, become expected.
63 Although visually guided movements should theoretically account for such uncertainty and volatility
64 statistics (Arthur et al., 2020; Beesley et al., 2015; Domínguez-Zamora et al., 2018), it remains

65 unclear how gaze behaviours are adjusted during complex visuomotor skills. Specifically, do agents
66 minimise prediction error in a progressive, Bayes-optimal manner over time? Or do they show
67 abrupt step-changes in visuomotor control under conditions of environmental uncertainty, where
68 gaze is directed to more strategic, non-linear spatial locations?

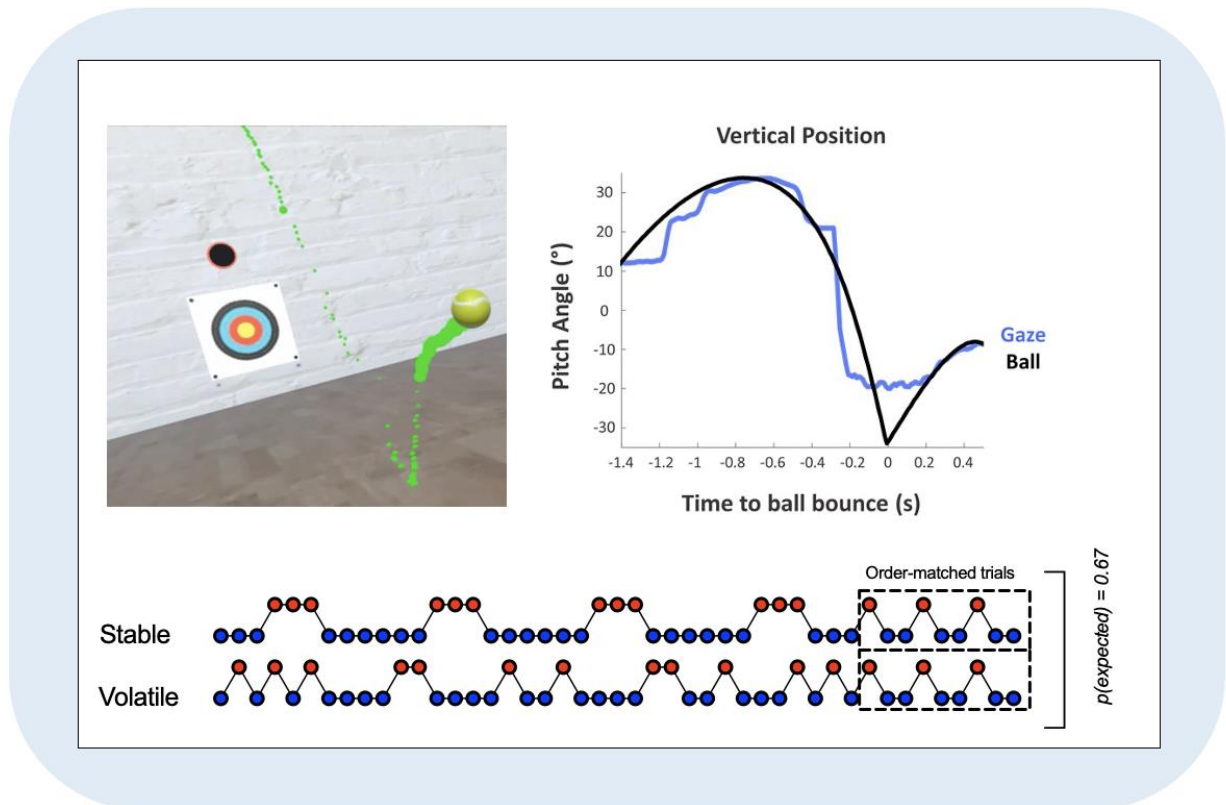
69 A further consideration relating to environmental uncertainty is its effect on learning. The
70 rate of associative learning should be enhanced for stimuli whose consequences are uncertain
71 (Dayan & Yu, 2003), as larger and more frequent prediction errors cause the generative model to be
72 revised. Environmental volatility also modulates the rate at which prior models are updated
73 (Behrens et al., 2007). The assimilation of new observations with prior expectations is weighted such
74 that strong priors resulting from lifelong learning (e.g., gravity; Zago et al., 2004)) are not easily
75 modified. Under stable conditions, it would be sub-optimal for a single aberrant event to reshape
76 these predictions. However, under volatile conditions it is necessary for top-down predictions to be
77 more easily modified in light of new observations, resulting in a functionally increased learning rate.
78 Indeed, learning from expected uncertainty and unexpected uncertainty may even be signalled via
79 different neuromodulators, with acetylcholine and norepinephrine performing these two respective
80 roles (Yu & Dayan, 2005). We would, therefore, expect predictive visual behaviours to be updated
81 more rapidly in the context of more unpredictably changeable environmental probabilities. This
82 hypothesis is yet to be empirically examined and is the objective of this paper.

83 Consequently, the present work sought to understand how unpredictable environmental
84 changes affect visuomotor control during naturalistic and unconstrained interceptive actions.
85 Further, we sought to test whether such changes approximate Bayes-optimal behaviour, as
86 predicted by active inference accounts of perception and action (Friston et al., 2016; Parr & Friston,
87 2019). To do this, we studied a virtual racquetball task (see Fig 1), in which participants typically
88 display strong prediction-driven gaze behaviours (Arthur et al., 2020; Diaz, Cooper, Rothkopf, et al.,
89 2013; Mann et al., 2019). In line with active inference approaches, it was hypothesised that: i)
90 performers will adjust predictive gaze behaviours between stable and volatile trials in a Bayes-
91 optimal fashion, such that they will place less weight on top-down predictions under volatile
92 conditions; ii) performers will show an adjusted learning rate, such that gaze behaviours will be
93 more strongly influenced by recent context under volatile trial conditions; and iii) environmental
94 shifts that are more unexpected will create a further increase in learning rate (i.e., for unexpected
95 uncertainty compared to volatility; see Bland & Schaefer, 2012).

96 **2. Methods**

97 **2.1. Experimental task and procedures**

98 Behavioural data were primarily collected in the context of understanding how
99 environmental uncertainty and volatility are processed in Autism Spectrum Disorder and a detailed
100 description of all experimental procedures are provided in an accompanying manuscript (Arthur et
101 al., 2020). As a result, no part of the study procedures or analyses were pre-registered prior to the
102 research being conducted. We report how we determined our sample size, all data exclusions, all
103 inclusion/exclusion criteria, all manipulations, and all measures. In short, the interception task took
104 the form of a VR racquetball (squash) game, in which participants had to return a bouncing ball back
105 towards a target on the wall (videos available online: <https://osf.io/qjbf2/>). The task was developed
106 using the gaming engine Unity (Unity Technologies, San Francisco, CA) and presented to participants
107 via an HTC Vive head-mounted display system (HTC Inc., Taoyuan City, Taiwan; Fig 1). Movements of
108 the headset and hand controller were monitored at 90Hz, based on positional detection in relation
109 to two infra-red 'lighthouse' tracking stations, while gaze was monitored at 120 Hz via an inbuilt
110 Tobii eye-tracking system (spatial accuracy: 0.5°). A virtual racquet was animated based on the
111 movement of the handheld controller, while the simulated court was a 15m square room with an
112 aiming target projected onto the front wall (see Fig 1). Virtual balls visually resembled those used in
113 real tennis, and were launched from just above the aiming target, along the midline of the room
114 (which was 0.75m away from participants on their 'forehand' side). All balls had the same *pre-*
115 *bounce* flight trajectory and speed, which were both consistent with the effects of gravity (-9.8m/s^2).
116 Participants were instructed to hit balls back towards the centre of the target on the front wall.



117

118 **Fig 1.** Virtual racquetball task. Participants intercepted bouncing balls in the virtual environment (top
 119 left; here shown with gaze point overlaid) using a tracked hand controller while wearing an HTC Vive
 120 Head-mounted display. The presented balls had identical visual appearance, pre-bounce flight
 121 trajectory, and speed but were given differing elasticity profiles that either corresponded with real
 122 tennis balls (i.e., expected), or were unusually bouncy (i.e., unexpected). In the ‘stable’ condition,
 123 balls were presented in a predictable serial order (cue-outcome congruency fixed at 66.67%),
 124 whereas under ‘volatile’ conditions, cue-outcome probabilities were unpredictably changeable,
 125 switching irregularly between highly- (83%), moderately- (67%) and non-predictive (50%) blocks
 126 (bottom). Both conditions ended with nine probability- and order-matched trials. The top right panel
 127 illustrates typical ball and eye trajectories for a single trial, as has been observed previously (Diaz,
 128 Cooper, & Hayhoe, 2013; Mann et al., 2019): after pursuing early-flight trajectory, gaze shifts ahead
 129 of the ball to a location just above the expected future bounce point (150-190ms), the location of
 130 which is sensitive to expectations of ball elasticity (Diaz, Cooper, Rothkopf, et al., 2013). After the ball
 131 has ‘caught up’, the eyes attempt to track the ball towards the racquet through a combination of
 132 smooth pursuit and corrective saccadic shifts (Diaz, Cooper, Rothkopf, et al., 2013; Land & McLeod,
 133 2000; Mann et al., 2013; Mann et al., 2019; Mrotek & Soechting, 2007).

134 Balls presented in each trial were of two possible types – expected and unexpected – which
135 corresponded to two different elasticity profiles. In *expected* trials, ball elasticity was set at 65%,
136 corresponding with the normal behaviour of a real tennis ball. For *unexpected* trials, elasticity was
137 increased to 85%; an easily detectable change in ‘bounciness’ and post-bounce trajectory (Arthur et
138 al., 2020; Diaz, Cooper, & Hayhoe, 2013). Crucially, the unnatural ball elasticity profile in the
139 unexpected trials was designed such that it deviated substantially from any prior real-world
140 experience of ball bounciness. Since pre-bounce ball trajectories were the same for all trials, ball
141 elasticity information could only be obtained from these distinct post-bounce ball trajectory profiles.
142 Before performing the task, participants received no information about these experimental
143 manipulations of ball elasticity, they were simply informed that the ball would bounce once and that
144 they were free to hit it at any point after this event.

145 By manipulating the frequency of presentation of the different ball elasticity profiles we
146 created stable and volatile conditions. Under stable conditions balls were presented in a predictable
147 serial order with cue-outcome congruency fixed at 66.67% (i.e., two thirds of balls were expectedly
148 bouncy and one-third unexpectedly bouncy). Under volatile conditions, cue-outcome probabilities
149 were made unpredictably changeable (i.e., unexpected uncertainty) by switching irregularly
150 between highly- (83%), moderately- (67%) and non-predictive (50%) trials in blocks of 6, 9 or 12 (trial
151 order sequences available from <https://osf.io/ewnh9/>). Crucially, each condition contained an
152 equivalent number of expected (n=30) and unexpected (n=15) trials, ensuring that the marginal
153 probability was identical, and conditions differed only in environmental volatility. Each 45-trial
154 condition took approximately 10 mins to complete and conditions were separated by a short
155 comfort break.

156 To enable within-condition comparisons of different levels of uncertainty, three expected
157 and three unexpected “test” trials were situated within each block. These trials had identical prior
158 cue-outcome contingencies (66.67%) and identical trial histories (n–1 were all expected trials).
159 Additionally, in order to compare environmental shifts and make learning rate comparisons, the final
160 nine trials in each of the stable and volatile blocks were “order-matched”. While these nine trials
161 matched the cue-outcome congruency in the rest of the stable condition, they represented an
162 unexpected shift away from the previously serial trial orders. In the volatile condition, however, they
163 effectively continued both the probability contingencies and volatile presentation order. This
164 allowed us to distinguish unexpected uncertainty from environmental volatility (Bland & Schaefer,
165 2012).

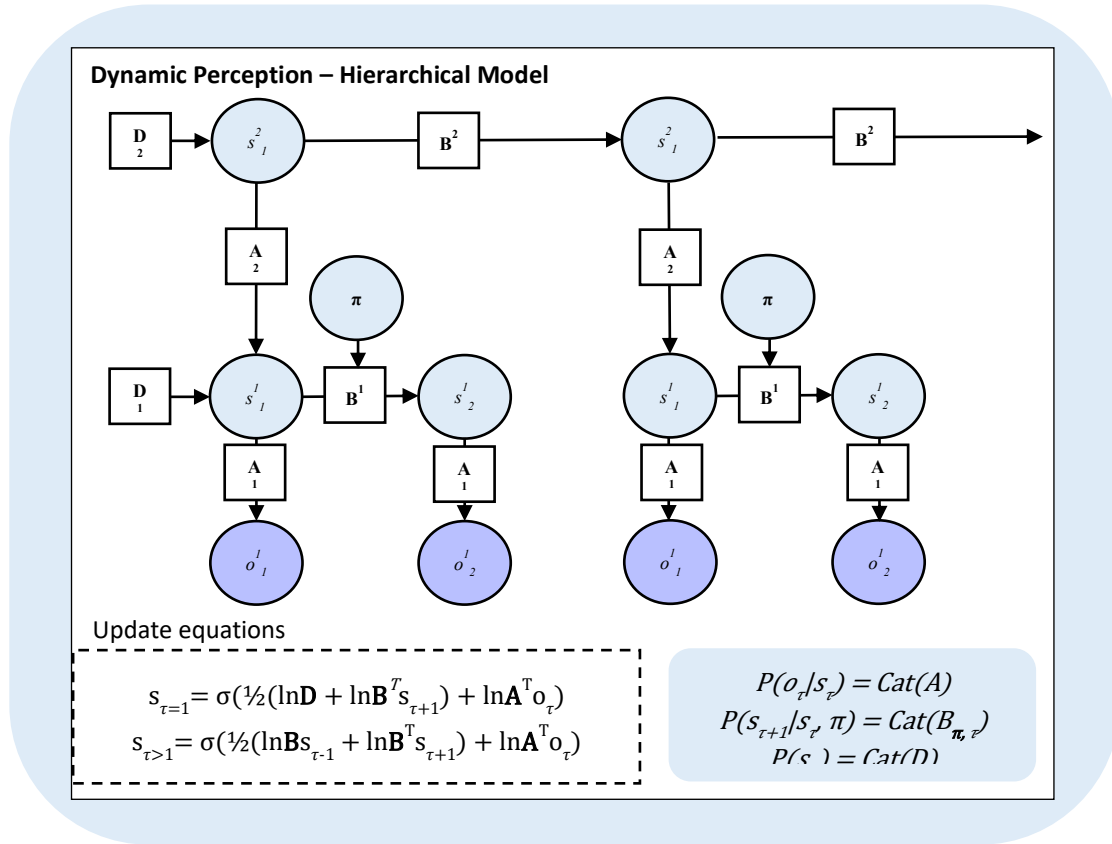
166 2.2. Participants

167 57 participants who did not have a history of musculoskeletal or neurological disorders
168 completed the study (34 male, 23 female; mean age: 22.05 ± 3.51 years; 91.23% right-handed). A
169 power analysis indicated that 50 participants were sufficient to detect effects of $d=0.7$ with 98%
170 power, $d=0.5$ with 80% power, and $d=0.3$ with 65% power, given $\alpha=.05$ in a two-tailed paired t-test
171 (power curves for a range of effect sizes and sample sizes are available online at
172 <https://osf.io/9exfk/>). Three participants were excluded from the study due to poor quality eye
173 tracking and/or incomplete data, leaving a sample of $n=54$. Prior to completing the stable or volatile
174 conditions, these participants provided written informed consent and were familiarised with the VR
175 procedures. During this time, gaze was calibrated over five virtual locations, a process subsequently
176 repeated upon any obvious displacement of the headset during trials. Participants then began by
177 completing six practice trials on the interception task, before undertaking both experimental
178 conditions in a counterbalanced order. Practice balls were projected from the target without a
179 bounce to ensure that ball elasticity remained unknown. Participants were all naïve to the
180 experimental aims, had no prior experience playing VR-based racquet sports, and received no visual
181 or haptic feedback in relation to racquet-ball contact. The study received approval from the School
182 of Sport and Health Sciences Ethics Committee (University of Exeter, UK) and Department of
183 Psychology Ethics Committee (University of Bath, UK).

184 2.3. Simulation modelling analysis

185 To simulate statistically-optimal behaviour in this task, we employed a Bayesian generative
186 model of perception derived from the Markov decision process (MDP) formulation of active
187 inference (Da Costa et al., 2020). In general terms, this simulation modelling was used to illustrate
188 the type of belief updating that would occur under Bayesian inference. The model takes a set of
189 initial parameters specified by the experimenter – e.g., prior beliefs about ball bounciness and rate
190 of learning – then iteratively updates beliefs (according to Bayes rule) following predefined
191 observations (observed ball bounces) and determines the action choices a Bayes-optimal agent
192 should make. The POMDP used here solves the otherwise intractable integrals required for model
193 inversion (i.e., moving from prior to posterior beliefs) through estimating posteriors over states via
194 an optimization routine (gradient descent) that seeks to minimise free energy in the model. This is
195 achieved by combining categorical prior expectations about states (**D**) and transitions between
196 states (**B**) with observed instances via the likelihood matrix (**A**), which maps the probability of hidden
197 states given observed instances (see Table 1 for descriptions of model parameters). Consequently,
198 the outputs of the model are estimated beliefs about the bounciness of future balls (i.e., the ‘hidden
199 state’) and the action choices that agents make based on that belief. For more details on the

200 mathematical formalism of these models, see Friston et al. (2017), Smith et al. (2020), or an
 201 introductory review by Smith and colleagues (2021).



202
 203 **Fig 2.** Bayesian network representation of two-level POMDP model. This POMDP model combines
 204 categorical prior expectations about states and transitions with observed instances via the likelihood
 205 matrix. Circles ('nodes') correspond to variables: s =state, o =observations, π =action policies. Squares
 206 are factors mediating the conditional relationships and take the form of matrices in the model:
 207 A =likelihood mapping between states and outcomes (i.e., $(o_{\tau}|s_{\tau})$), D =initial state priors (i.e., (s_1)),
 208 B =state transition matrices encoding beliefs about how hidden states evolve over time (i.e.,
 209 $(s_{\tau+1}|s_{\tau})$). Observation and state subscripts correspond to time point in a trial (τ). Importantly, when
 210 $\tau>1$, the B matrix from $\tau-1$ functions as an empirical prior, playing the same role as the D vector at
 211 $\tau=1$. Arrows connecting nodes indicate dependencies between variables. Sigma (σ) in the update
 212 equations refers to a SoftMax function (normalized exponential), which allows vector values to make
 213 up a proper probability distribution. The lower level of the model (superscript 1) represents
 214 probability updating at the trial level, whereas the higher level (superscript 2) represents learning
 215 about trial sequences. Consequently, D^1 represents a prior over the probability of normal versus
 216 bouncy balls, while D^2 represent a prior over the stability of those probabilities over time.

217

218 To specifically index uncertainty and volatility estimations, we computed a generative model
219 with a hierarchical or ‘deep temporal’ structure. Here, the lower model encodes probability updating
220 during a single trial and from one trial to the next, while the higher model encodes patterns of
221 observations over longer trial sequences. An illustration of this process is provided in Fig 2.
222 Observations (o) in the lower level POMDP model were categorical and included a start observation,
223 the appearance of the ball, an expected ball bounce profile, and an unexpectedly high bounce
224 profile. Although participants were required to hit the ball with their racquet, the observation of
225 bounciness was made before the hit, hence the model effectively encodes up until hit point. The
226 lower-level trials formally had three timesteps ($\tau = 1$ [start], $\tau = 2$ [ball appearance], and $\tau = 3$
227 [bounce observation]) while higher-level trials operated over blocks of nine trials. The agent began
228 in the “start” state and made the associated “start” observation, then either observed a normal
229 bounce, or an unexpectedly high bounce. It was modelled that they then inferred a posterior
230 distribution over states that assigned a probability to the normal/high bounciness state, informed by
231 prior beliefs about the likelihood of observing a normal versus a bouncy ball and the mapping
232 between observations and states. Crucially, these lower-level observations updated priors at the
233 higher level, where expectations of environmental stability were represented. As a result, the
234 higher-level model encodes a form of ‘meta-uncertainty’ (i.e., volatility) about changing patterns of
235 uncertainty or deviation from an expected order.

236 These simulations reflect an instrumental use of modelling to generate qualitative
237 predictions about Bayes-optimal behaviour, rather than a veridical representation of psychological
238 processes. Plausible prior models for $p(\text{expected})$ and $p(\text{stability})$ were specified, but the true
239 strength of participants’ prior expectations is unknown. Lifelong learning about credible ball bounce
240 profiles means that participants likely had a strong prior favouring the expected ball. However, the
241 virtual nature of the task and the experimental setting could mean that despite lifelong learning
242 about ball bounciness, expectations were somewhat weaker (e.g., see Zago et al., 2004). Therefore,
243 a prior was selected to encode a belief that the expected ball was 99 times as likely as the
244 unexpected ball. The distribution over this belief was set to indicate that this belief was fairly weak
245 (i.e., low precision or confidence). Priors for categorical outcomes are represented in the model as
246 Dirichlet distributions, a multivariate generalization of the beta distribution which is defined over a
247 vector of values that sit on the interval $[0,1]$, and sum to one. Therefore a 99 to 1 belief can be
248 represented as a relatively stronger $[99,1]$ or weaker $[0.99,0.1]$ distribution. We specified a prior
249 belief over bounciness of $[9.9, 0.1]$ at the lower level and an even prior belief over stable/volatile $[5,$
250 $5]$. Fifty simulated participants were then modelled for our analyses, with a degree of stochasticity in
251 action selection.

252 **Table 1.** Description of computational model elements

Model variable	General definition	Model-specific definition
τ	Timepoint within a trial	At $\tau=1$ agent was modelled as waiting to observe the ball, at $\tau=2$ the ball appeared, at $\tau=3$ either a normal or bouncy ball was observed and a posterior probability about ball bounciness was inferred.
o_τ	Observable outcomes at time τ	<ol style="list-style-type: none"> 1. Start 2. Ball appearance 3. Normal bounce 4. High bounce
s_τ	Hidden states at time τ	<ol style="list-style-type: none"> 1. Start 2. Ball appearance 3. Normal bounciness 4. High bounciness
A matrix ($p(o_\tau s_\tau)$)	Matrix encoding beliefs about the relationship between hidden states and observable outcomes (i.e., the likelihood)	Beliefs about the relationship between the observed bounciness and the hidden state of bounciness. In this instance the observation provides perfect evidence for the state.
B matrix ($p(s_{\tau+1} s_\tau)$)	Matrix encoding how beliefs about states will evolve over time	Encodes the prior beliefs about whether a normal or bouncy state would occur on each trial
D vector ($p(s_{\tau=1})$)	Matrix encoding beliefs about initial hidden states	Initial belief
π	Action policy	Action to anticipate an expected or unexpected ball (i.e., predictive gaze).
<i>Free parameters used during model fitting</i>		
α	Action precision	Parameter that controls how random action selection is after a policy has been chosen. Higher values indicate deterministic behaviour.
η	Learning rate (eta)	Parameter from 0-1 that scales the size of the update to beliefs at each time point.
RS	Risk seeking	Parameter encoding how strong the preference is to predict the correct outcome
LA	Loss aversion	Parameter encoding how strong the preference is for not predicting the incorrect outcome

253

254

255 2.4. Gaze data analysis

256 Data extraction and cleaning procedures are described in an accompanying paper (Arthur et
257 al., 2020). Here, participant's cyclopean gaze vector and head position (x,y,z) were recorded from
258 the virtual environment and plotted with respect to 2D direction in space, to provide relative 'in-
259 world' angular orientations (head-ball, gaze-head, and gaze-ball angles). Gaze fixations were
260 detected using a spatial dispersion algorithm (Krassanakis et al., 2014) where fixation events were
261 defined as clusters of successive gaze points within 3° for >100ms, and where gaze velocity was <
262 30°/s (as in Diaz, Cooper, & Hayhoe, 2013). Saccades were defined as portions of data where gaze
263 acceleration (°/s²) exceeded five times its median absolute acceleration value (as in Mann et al.,
264 2019). To remove any potential artefacts resulting from tracking loss, an additional filter was applied
265 whereby the velocity of saccades had to exceed 40°/s for five consecutive frames and be at least
266 20% greater than that of the ball. For trials where this automated acceleration criteria did not
267 identify any anticipatory pre-bounce saccades, trials were manually inspected using a 30°/s velocity
268 threshold (Cesqui et al., 2015). Saccade onset and offset times were determined from acceleration
269 minima and maxima (Fookien & Spering, 2020).

270 The following prediction-related metrics were extracted from this data: the onset of the pre-
271 bounce saccade; the pitch angle of the pre-bounce fixation; and an index of surprise calculated from
272 the unexpected-expected (UE-E) gaze tracking difference. The onset of the pre-bounce saccade was
273 used to index how early the predictive fixation was initiated. Pitch angle indicates the spatial
274 position of the predictive fixation with elevated positions indicating the prediction of bouncer
275 trajectories (Arthur et al., 2020; Diaz, Cooper, & Hayhoe, 2013). Since both of these outcome
276 variables refer to pre-bounce gaze events (that occur before post-bounce sensory information can
277 be obtained), they are driven by an agent's prior expectations about ball elasticity and
278 environmental stability. However, to probe the effects of unexpected outcomes and their levels of
279 associated 'surprisal' we examined the UE-E gaze tracking difference, which was calculated from a z-
280 score of the average post-bounce gaze-ball pitch difference (vertical plane) for each participant.
281 Mean values on expected trials were subtracted from their corresponding unexpected test trial
282 values, such that higher scores indicated a greater difference between expected and unexpected
283 trials (i.e., greater behavioural 'surprise'; Arthur et al., 2020; Baldi & Itti, 2010).

284 Statistical analysis was conducted using JASP 0.12.1 (JASP team, 2018). Univariate outliers
285 ($p < .001$) for gaze and kinematic variables were identified and removed from the analysis. Four
286 participants with data identified as outliers were excluded from gaze analysis (remaining $n=50$). Poor
287 quality ball tracking was identified in a further two participants at this stage, and UE-E difference
288 scores were consequently removed for these cases. Group comparisons were conducted using

289 Students t-test, or a Wilcoxon signed rank test in cases where data significantly deviated from
290 normality. Cohen's d was used to quantify effect size for student's t-test, and the rank biserial
291 correlation¹ (r_{rb}) for Wilcoxon signed rank test. Conclusions were primarily based on significance
292 values, but Bayes factors (BF_{10}) were also calculated to further illustrate the evidence for the
293 alternative versus the null. We used a symmetric Cauchy prior distribution, which was centred on
294 zero with a width parameter of 0.707 (corresponding to an 80% probability that the effect size (d)
295 lies between -2 and 2). We follow the convention that $BF_{10}>3$ indicates moderate support for the
296 alternative model and $BF_{10}>10$ indicates strong support (van Doorn et al., 2019). All data from this
297 experiment is freely available and can be accessed from the Open Science Framework
298 (<https://osf.io/h5nu7/>).

299 **2.5. Learning rate analysis**

300 By fitting a POMDP model to real participant data, we were able to identify a set of
301 parameters that enable model predictions to best match observed behaviour (i.e., maximising
302 (*participant behavior* | *model*)). In contrast to the model simulations described above, which
303 predict actions from initial model parameters, here we work backwards from observed behaviours
304 to determine the model parameters that would best explain those actions. In this way, we can
305 estimate the values of pre-specified free parameters (e.g., learning rate) that may vary between
306 participants or conditions. Specifically, we estimated learning rate over the lower level of the model
307 described in Fig 2 which denotes the trial-by-trial perception. While both flat and hierarchical
308 models have been found to explain learning in different tasks (Heilbron & Meyniel, 2019), a simple
309 flat model was chosen here to address the primary question about learning rate while avoiding
310 additional assumptions about hierarchical perception. For instance, unexpected uncertainty
311 represented at a second level could be encoded via tracking unexpected changes in marginal
312 probabilities *or* via beliefs about the wider volatility of the environment (as in our simulations; Fig. 3;
313 Mathys et al., 2014; Meyniel et al., 2015). A single level model negated the need for these additional
314 assumptions which would influence model behaviour. By searching through different possible
315 combinations of parameter values, the best combination can be found for a given participant.
316 Parameter estimation was achieved using variational Bayes (Friston et al., 2007), which works from a
317 set of estimated prior values over parameters and performs gradient descent on VFE in a similar
318 manner to the POMDP (Smith et al., 2021). After obtaining parameter estimates for real participants,
319 we checked the 'parameter recoverability' of the model, i.e., could the model accurately estimate
320 values that were used to generate some artificial data. After simulating data from a range of learning

¹ Glass(1966) recommends that the rank biserial correlation is treated as approximate to Pearson's correlation for the interpretation of effect size.

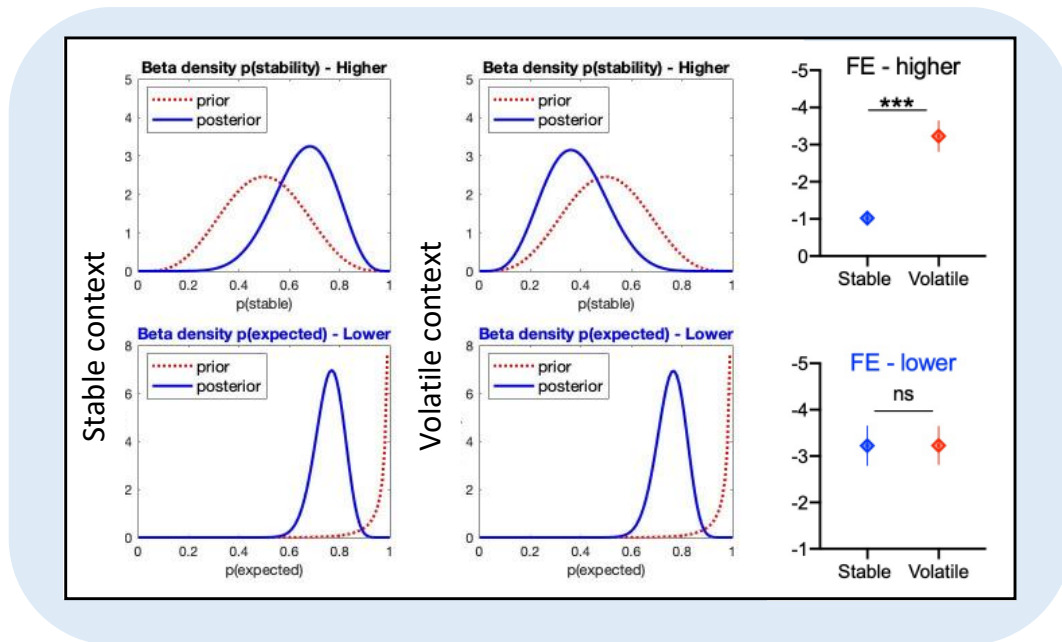
321 rate values, we subsequently refit the model to the simulated data to ensure the parameter
322 estimates converged on the known values. Model checks showed good recoverability (plots available
323 in the online files; <https://osf.io/h5nu7/>).

324 To obtain the best fit of the model, we enabled four free parameters and compared model
325 fits with different combinations of these parameters. The free parameters were learning rate,
326 sensitivity to reward, sensitivity to loss, and ‘action precision’, a value which encodes the extent to
327 which action choices are deterministic or random. Successive POMDP models with different free
328 parameter combinations were compared using a Bayesian random effects model (spm_BMS.m
329 function: Statistical Parametric Mapping 12 toolbox; Wellcome Trust Centre for Neuroimaging,
330 London, UK, <http://www.fil.ion.ucl.ac.uk/>), which assesses the VFE of each model fit and returns the
331 relative probabilities (e.g., [0.9, 0.1]) of the better fit (the protected exceedance probability; Rigoux
332 et al., 2014). As it has been shown that the pitch angle of the bounce fixation is adjusted in line with
333 previously observed ball bounciness (Diaz, Cooper, & Hayhoe, 2013), pitch angle was used to index
334 beliefs about ball bounciness. Lower locations were taken to indicate a belief that $p(\text{expected})$ was
335 more likely. Pitch angle was discretised for modelling purposes: when gaze was shifted to a higher
336 location than on the previous trial ($>1\text{SD}$ change) this was taken as a shift towards higher
337 $p(\text{expected})$ and vice versa. To maintain the trial orders, participants with $<15\%$ missing values had
338 pitch angle imputed using a linear moving average (median) imputation (Cole, 2008; Moritz & Bartz-
339 Beielstein, 2017). Less than 15% missing values corresponded to $>95\%$ imputation efficiency, as
340 recommended by Cole (2008). Participants with $>15\%$ missing data were excluded, resulting in 42
341 datasets for the learning rate analysis.

342 3. Results

343 3.1. Simulation modelling results

344 The results of POMDP simulations with 50 Bayes-optimal agents are presented in Fig 3. At
345 the lower level of the model there was no difference in free energy between stable and volatile
346 conditions as the marginal probability for $p(\text{expected})$ remained equivalent. However, at the higher
347 level of the model (beliefs about volatility), agents exhibited larger prediction errors in the volatile
348 compared to the stable context and shifted away from a belief in stability. During dynamic
349 visuomotor actions this additional uncertainty should induce a higher learning rate and greater
350 weighting of recent context. If human agents adjust beliefs in a Bayes-optimal fashion and seek to
351 minimise free energy through their visual sampling, as predicted by active inference, a greater
352 weighting of recent context and higher learning rate should be observed in predictive visual
353 behaviours.



354

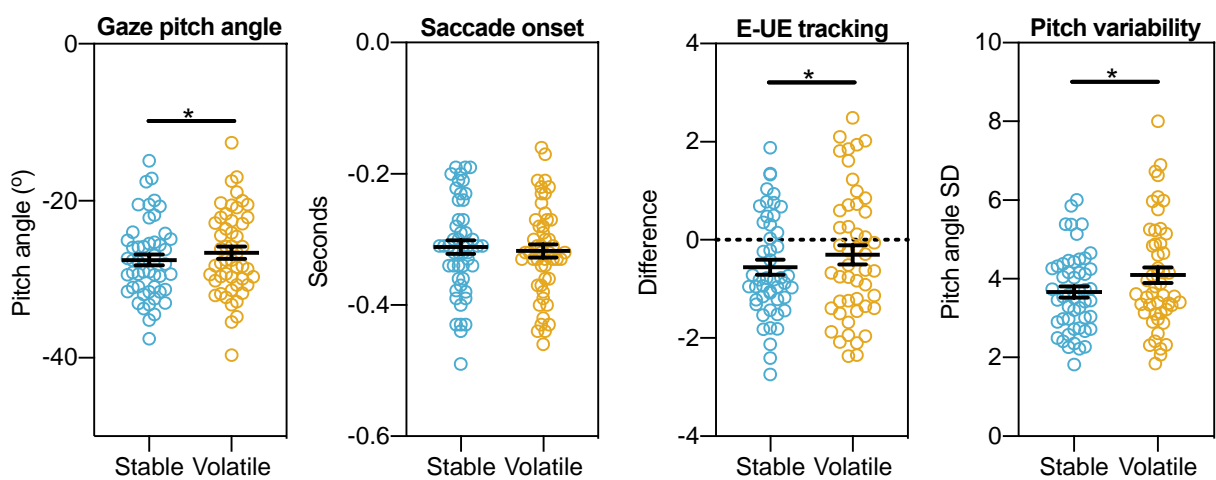
355 **Fig 3.** POMDP simulation results. Figures to the left and centre are prior and posterior beta density
 356 plots for expectations about context ($p(\text{stable})$ for the higher level of each model) and ball elasticity
 357 ($p(\text{expected})$ for the lower level of each model). Plots to the right are total model free energy (means
 358 and 95% confidence intervals) over trials at the higher and lower levels for stable contexts (note:
 359 more negative indicates greater free energy). Plots indicate group. *** $p < .001$, ns=non-significant.

360 3.2. Behavioural results

361 To investigate whether agents adjust visuomotor control in a Bayes-optimal fashion, we
 362 extracted key prediction-related gaze variables from the racquetball dataset. According to the
 363 simulated models above, Bayes-optimal agents should place less weight on top-down predictions
 364 when forming their beliefs under volatile conditions. When extended to the behaviour of real
 365 participants, this could manifest in a later onset of the pre-bounce saccades and/or smaller
 366 distinctions in post bounce tracking between expected and unexpected balls (i.e., lower UE-E
 367 difference scores). Furthermore, greater prior to posterior shifts in the volatile context (i.e., greater
 368 weighting of recent context) should be reflected in higher pre-bounce fixation positions (pitch
 369 angles), which are more frequently adjusted (i.e., highly variable) over time.

370 A Wilcoxon signed-rank test indicated no difference in the timing of the onset of the
 371 predictive saccade ($W = 606$, $p = .32$, $r_{\text{rb}} = 0.17$), with the Bayes factor favouring the null ($\text{BF}_{10} = 0.27$).
 372 However, analysis of the pre-bounce fixation showed that the pitch angle of gaze was different
 373 between stable and volatile conditions, in spite of their equivalent cue-outcome probabilities (Fig 4).
 374 Specifically, a paired Student's t-test indicated significantly higher pitch averages in the volatile
 375 condition ($M = -26.6$, $SD = 5.5$) compared to the stable condition ($M = -27.5$, $SD = 4.95$; $t(49) = 2.52$, p

376 = .02, $d = 0.36$), although the Bayes Factor was only weakly supportive ($BF_{10} = 2.67$). This tendency to
 377 predictively position gaze at a higher location (under more volatile trials) seemingly affected post-
 378 bounce ball tracking responses. Here, Student's t-tests indicated a marginally significant reduction
 379 in E-UE difference for the volatile condition ($M = -0.30$, $SD = 1.32$) compared to the stable condition
 380 ($M = -0.56$, $SD = 1.05$; $t(47) = 2.02$, $p = .049$, $d = 0.29$), but the Bayes factor was inconclusive ($BF_{10} =$
 381 1.01). Supplementary Analysis showed that swing kinematics were also adapted between conditions,
 382 with participants generally restricting their range of motion in more volatile trials (Supplementary
 383 Fig 1). Therefore, participants appeared to adjust both their *weighting* and *updating* of predictions in
 384 a dynamic, Bayes-optimal manner.



385

386 **Fig 4.** Interceptive gaze Behaviours. *Dot plots (with mean and standard error) comparing eye*
 387 *movement variables between stable and volatile conditions. Note: * $p < .05$.*

388 However, the degree to which these visuomotor patterns are Bayes-optimal required further
 389 scrutiny. It is possible that participants may be responding to environmental volatility using *non-*
 390 *linear* behavioural strategies, as opposed to context-sensitive modulations predicted by active
 391 inference. An example of this could be ‘centring’ strategies, where gaze is positioned mid-way
 392 between two outcome possibilities (e.g., see Heinen et al., 2005). Crucially, such a strategy is
 393 characterised by a rapid step-change in behaviour, as opposed to a more gradual prior-driven
 394 adjustment over time. Hence, in stark contrast to dynamic Bayesian updating (which should be
 395 highly variable under volatile conditions), stimulus ordering should have little effect on non-linear
 396 behavioural strategies. To rule out a centring strategy, we therefore analysed pitch angle *variability*.
 397 A paired t-test indicated significantly lower within-subject standard deviations in position for stable
 398 ($M = 3.67$, $SD = 1.00$) compared to volatile conditions ($M = 4.09$, $SD = 1.39$; $t(49) = 2.31$, $p = .025$, $d = 0.33$),
 399 although the Bayes Factor provided only weak support ($BF_{10} = 1.72$). Therefore, under volatile

400 conditions, it appears that participants may have made more variable and dynamic adjustments to
401 pitch angle, rather than just maintaining a generic, non-linear behavioural strategy.

402 3.3. Learning rate analysis

403 Finally, the POMDP model developed during simulations was fitted to the real participant
404 data to estimate parameters for participants' learning rate, prediction errors, and beliefs about ball
405 elasticity. The model was based on gaze pitch angle; a previous indicator of bounciness expectations
406 (Diaz, Cooper, Rothkopf, et al., 2013). This estimation was achieved using variational Bayes (Friston
407 et al., 2007), whereby model parameters are optimised for the behaviour of each individual using
408 gradient descent. A best fitting POMDP model was subsequently identified, which contained free
409 parameters for an overall learning rate estimate (η), an action precision parameter (α), and a
410 parameter encoding loss aversion. This model predicted behaviour to a high degree – the probability
411 of the true action being the one predicted by the model was 0.83. Parameter recoverability (i.e., the
412 ability of the model to accurately estimate, or recover, artificially imputed values) was assessed by
413 simulating data based on known parameters, then re-estimating those parameters from the data.
414 Recoverability was found to be moderate to good, with correlations of $r = 0.4, 0.5,$ and 0.7 between
415 true and estimated parameters for alpha, eta, and loss aversion (for further details on model
416 selection and checks of fit see <https://osf.io/h5nu7/>).

417 Firstly, we examined the blocks of stable and volatile trials (excluding the 9 order-matched
418 trials at the end) which varied in order predictability but had equivalent cue-outcome contingencies.
419 Paired t-tests showed that there was no difference in the overall learning rate parameter (η)
420 between stable ($M = 0.52, SD = 0.18$) and volatile blocks ($M = 0.53, SD = 0.15; t(41) = -0.36, p = .72, d$
421 $= 0.06$), and the Bayes factor supported the null ($BF_{10} = 0.18$). Nor was there a difference in free
422 energy over likelihood beliefs between stable ($M = 0.03, SD = 0.01$) and volatile blocks ($M = 0.03, SD$
423 $= 0.01; t(41) = -0.43, p = .67, d = 0.07, BF_{10} = 0.18$). There was also no difference in free energy over
424 transition beliefs between stable ($M = 0.01, SD = 0.001$) and volatile blocks ($M = 0.01, SD = 0.001;$
425 $t(41) = -0.02, p = .98, d = 0.004$), with the Bayes factor again supporting the null ($BF_{10} = 0.17$).

426 Next, we modelled the nine order-matched trials that followed stable and volatile blocks.
427 These 'matched' trials were essentially a continuation of the volatile block (i.e., unknown order), but
428 represented a sudden shift from the predictable serial order of the stable condition. Hence they
429 provided a comparison of volatility and unexpected uncertainty (Bland & Schaefer, 2012). Paired t-
430 tests indicated that the estimated learning rate parameter (η) was significantly higher following the
431 stable condition ($M = 0.55, SD = 0.05$) than the volatile condition ($M = 0.55, SD = 0.04; W(41) = 507, p$
432 $= .02, r_{rb} = 0.44$), but with a weakly supportive Bayes Factor ($BF_{10} = 1.20$). Free energy over the

433 likelihood was also higher for post-stable ($M = 0.036$, $SD = 0.001$) compared to post-volatile blocks
 434 ($M = 0.035$, $SD = 0.001$; $t(41) = 3.33$, $p = .002$, $d = 0.51$, $BF_{10} = 17.44$). Likewise, free energy over
 435 transition beliefs was significantly higher for post-stable ($M = 1.10 \cdot 10^{-2}$, $SD = 2.6 \cdot 10^{-4}$) compared to
 436 post-volatile blocks ($M = 1.04 \cdot 10^{-2}$, $SD = 5.03 \cdot 10^{-4}$; $W(41) = 645$, $p = .02$, $r_{rb} = 0.43$, $BF_{10} = 18.38$),
 437 indicating a larger updating of beliefs about likely sequences. Therefore, though we did not identify
 438 any overall differences in learning rate between stable and volatile conditions, there appeared to be
 439 significant between-condition differences in how gaze responses are updated in response to
 440 unexpected probability shifts (see Fig 5).

441

442

443

444

445

446

447

448

449

450

451

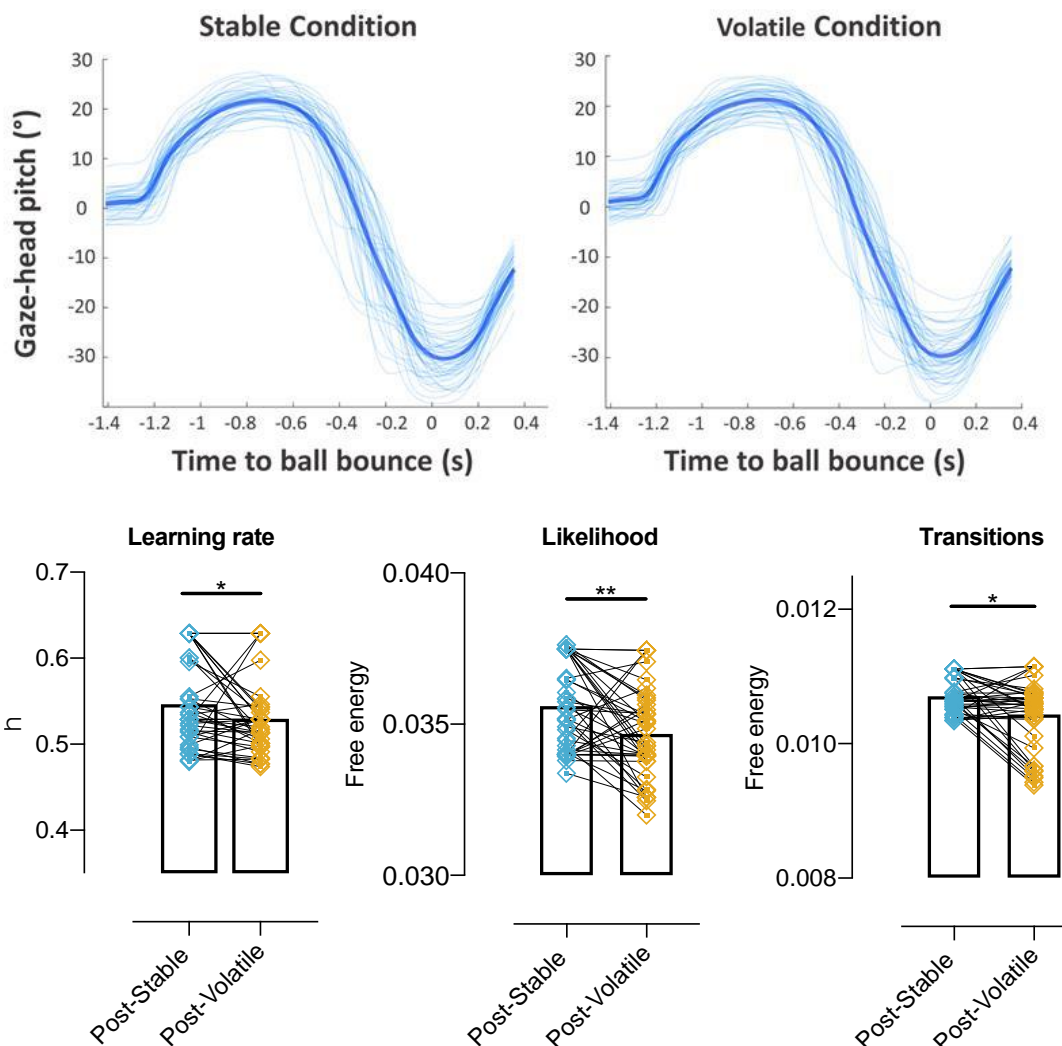
452

453

454

455

456



457 **Fig 5.** Gaze traces from stable and volatile conditions (top), with dot plots of POMDP parameter
 458 estimates showing the differences for post-stable (unexpected uncertainty) and post-volatile
 459 (continuing volatility) order-matched trials indicative of reduced surprisal and learning rate. Note:
 460 * $p < .05$, ** $p < .01$

461

4. Discussion

462

463

464

465

466

467

468

469

470

471

Predictive coding theories propose the minimisation of prediction error as a biologically plausible governing principle for perception (Friston, 2005; Rao & Ballard, 1999). Active inference extends free energy minimisation to action planning and selection as a mechanism to minimise Bayesian surprisal (Friston et al., 2016; Parr & Friston, 2019). This scheme generates a number of predictions about how the visual guidance of action should be affected by the uncertainty which arises from noisy sensory feedback, imperfect knowledge of the world, and changing environmental states. We examined these predictions of active inference theories in relation to visual guidance and motor execution in a volatile environment. Our findings extend the active inference framework beyond simple tasks and support it as a theoretical foundation for studying unconstrained visuomotor skills.

472

473

474

475

476

477

478

479

480

481

482

Hierarchical POMDP simulations of the racquetball task indicated that, for a Bayes-optimal agent, the volatile context should induce elevated prediction errors and a greater reliance on recent context, with posterior beliefs ($p(\text{expected})$) that were more weighted towards new observations. No change was observed in the onset of predictive saccades, suggesting that additional uncertainty arising from the volatile context did not affect temporal aspects of anticipatory gaze shifts. However, results showed that subsequent pre-bounce visual fixations were directed to a higher spatial position in the volatile context. This led to a reduction in post-bounce E-UE tracking difference (i.e., dampened surprisal), in a manner that is indicative of weaker prior expectations about 'normal' bounce trajectories. Together, these results suggests that participants used dynamic adjustments to predictive gaze behaviour to minimise tracking error from unexpected balls when they felt less certain about predicting likely outcomes.

483

484

485

486

487

488

489

490

491

492

493

494

In contrast to our predictions, our POMDP model indicated no overall difference in learning rate (indexed by shifts in gaze pitch angle) between the stable and volatile conditions. There was, however, increased *variance* in the pitch angle of the bounce fixation during the volatile condition, suggesting larger and more frequent adjustments of gaze position in the more uncertain context. The POMDP model did reveal differences in learning rate for the nine order-matched trials that followed the stable and volatile block sequences. Specifically, computationally 'surprising' trial order changes in the stable condition led to an increased learning rate and exaggerated updating of beliefs about ball transitions probabilities. Here, recent context was weighted more heavily following an unexpected shift in environmental probabilities (i.e., post-stable), compared to order matched trials that followed a period of already high volatility. These findings further support active inference accounts, and show an important difference in the response to unexpected uncertainty compared to volatility, as proposed by Bland and Schaefer (2012).

495 Active inference schemes suggest that optimal learning under unexpected uncertainty is
496 achieved through a hierarchical generative model which estimates shifting probabilities (Friston et
497 al., 2016; Meyniel et al., 2015). Our simulations (Fig. 3), for instance, encode dynamic beliefs about
498 environmental volatility (level 2) as well as marginal probabilities of ball bounce outcomes (level 1).
499 However, the exact nature of these context-sensitive higher-level mechanisms, and how they
500 influence learning rate, is unclear. Indeed, there have been proposals that volatility estimations are
501 also hierarchical in nature and that agents encode beliefs about the stability of this parameter
502 (Mathys et al., 2014). This raises the possibility that environmental volatility could itself be
503 considered more or less stable (see supplementary analyses). Moreover, while environmental
504 volatility has been conceptualised as a dynamic modulator of learning (Behrens et al., 2007),
505 changes in learning rate could be achieved through multiple hierarchical beliefs about higher level
506 encoding of volatility, or simple single-level (flat) learning models (Bell et al., 2016; Heilbron &
507 Meyniel, 2019; Meyniel et al., 2016; Wyart & Koechlin, 2016). Although our design did not allow us
508 to disambiguate hierarchical and flat model origins of learning rate changes (although see Heilbron
509 & Meyniel, 2019), the effect of the preceding sequence on learning rate (post-stable versus post-
510 volatile) suggests an awareness of a change point, and therefore appears to support a hierarchical
511 model of learning. Additional simulations using our hierarchical model predicted higher learning
512 rates following a volatile sequence, in contrast to our behavioural results (see supplementary
513 analyses for further discussion). Therefore, future research must establish precisely which higher-
514 level computations underpin active inference behaviours and how these estimates are encoded
515 across dynamic and hierarchical sensorimotor systems.

516 Our results suggest that not only did people update their expectations about likely ball
517 trajectories in a Bayes-optimal fashion, but that those predictions were reflected in adjusted
518 visuomotor coordination (see supplementary analyses). In addition to the gaze changes discussed
519 above, supplementary analyses highlighted clear changes in swing kinematics between stable and
520 volatile conditions. Specifically, ROM was significantly reduced in more volatile conditions, in a
521 manner that is suggestive of a ‘freezing’ of degrees of freedom. These kinematic changes seem to
522 reveal a regression towards a simpler movement pattern, whereby joint angles are ‘fixed’ as an
523 active attempt to minimise movement uncertainty (O’Sullivan et al., 2009). However, findings are
524 incompatible with ‘step-changes’ in visuomotor behaviour that would suggest deliberate strategic
525 policies. Instead, adjustments in gaze, motor, and learning profiles appeared to follow Bayesian
526 updating principles, whereby actions were progressively adapted in line with environmental
527 probabilities and the frequency with which these statistics changed.

528 It should be noted that the statistically significant gaze and kinematic effects we report are
529 relatively small (Cohen's $d=0.3-0.4$), particularly when contrasted with the large changes in prior
530 belief predicted by the POMDP simulations. However, visuomotor processes are inherently noisy
531 and impaired by imperfect sensory information (Körding & Wolpert, 2004), unlike the simulations.
532 That Bayes-optimal changes were detected across relatively few trials in noisy visual and motor
533 variables indicates that probabilistic context exerts an important influence on prediction in complex
534 visuomotor behaviours. Consequently, these relatively modest statistical effects could have
535 important theoretical and practical implications. In particular, the ability to make predictions from
536 prior models is fundamental to various high-performance domains, such as elite sport or military
537 combat. While theories of skilled anticipation in interceptive tasks have begun to identify the
538 importance of probabilistic context for action planning (Gray & Cañal-Bruland, 2018; Gredin et al.,
539 2018, 2020; Harris et al., 2021; Loffing & Cañal-Bruland, 2017; Runswick et al., 2020), the present
540 work illustrates how an active inference framework can extend this understanding. Specifically, our
541 findings demonstrate that unexpectedly changing probabilistic contexts will alter anticipatory
542 behaviours and result in greater weighting of recent context. Indeed, strong predictions can become
543 maladaptive in uncertain environments. Of note here then, is evidence that task experts (e.g., in
544 sport) might use prior probabilistic information to greater effect than novices (Gredin et al., 2020;
545 Runswick et al., 2020). Within an active inference framework, extensive task knowledge will
546 inevitably generate stronger priors leading to prediction-driven behaviour. However, future work
547 may wish to investigate whether the use of probabilistic context in real-world anticipation is entirely
548 driven by volume of experience (i.e., more precise prior) or if 'skill' somehow relates to more
549 judicious application of this prior knowledge.

550 **4.1. Conclusions**

551 The present work illustrated that predictive gaze behaviours, such as those made to
552 intercept a bouncing ball, are adjusted in a Bayes-optimal fashion in response to unexpectedly
553 changing or volatile conditions. This result extends our neurocomputational understanding of
554 dynamic motor tasks and highlights the potential of an active inference framework for studying
555 visually guided actions. In essence, when faced with unpredictably changing environmental
556 conditions, such as the tennis court becoming rough or a between-set change of balls, agents will
557 adjust their predictions in a statistically optimal fashion. This has important implications for theories
558 of skilled action (Gredin et al., 2020; Runswick et al., 2020), which have considered the influence of
559 probabilistic context (expected uncertainty) but are yet to outline the impact of unexpectedly
560 changing environments (volatility) on predictive visual behaviours.

561
562
563
564
565
566
567
568
569
570
571
572
573
574
575
576
577
578
579
580
581
582
583
584
585

References

- Abernethy, B., Gill, D. P., Parks, S. L., & Packer, S. T. (2001). Expertise and the Perception of Kinematic and Situational Probability Information. *Perception, 30*(2), 233–252.
<https://doi.org/10.1068/p2872>
- Arthur, T., Harris, D., Buckingham, G., Brosnan, M., Wilson, M., Williams, G., & Vine, S. (2020). *Expecting the Unexpected: An examination of active inference in autistic adults using immersive virtual reality*. PsyArXiv. <https://doi.org/10.31234/osf.io/x52ed>
- Baldi, P., & Itti, L. (2010). Of bits and wows: A Bayesian theory of surprise with applications to attention. *Neural Networks, 23*(5), 649–666. <https://doi.org/10.1016/j.neunet.2009.12.007>
- Beesley, T., Nguyen, K. P., Pearson, D., & Pelley, M. E. L. (2015). Uncertainty and predictiveness determine attention to cues during human associative learning. *The Quarterly Journal of Experimental Psychology, 68*(11), 2175–2199.
<https://doi.org/10.1080/17470218.2015.1009919>
- Behrens, T. E. J., Woolrich, M. W., Walton, M. E., & Rushworth, M. F. S. (2007). Learning the value of information in an uncertain world. *Nature Neuroscience, 10*(9), 1214–1221.
<https://doi.org/10.1038/nn1954>
- Bell, A. H., Summerfield, C., Morin, E. L., Malecek, N. J., & Ungerleider, L. G. (2016). Encoding of Stimulus Probability in Macaque Inferior Temporal Cortex. *Current Biology, 26*(17), 2280–2290. <https://doi.org/10.1016/j.cub.2016.07.007>
- Bernstein, N. A. (1967). *The control and regulation of movements*. London: Pergamon Press.
- Bland, A. R., & Schaefer, A. (2012). Different Varieties of Uncertainty in Human Decision-Making. *Frontiers in Neuroscience, 6*. <https://doi.org/10.3389/fnins.2012.00085>
- Cesqui, B., Mezzetti, M., Lacquaniti, F., & d’Avella, A. (2015). Gaze Behavior in One-Handed Catching and Its Relation with Interceptive Performance: What the Eyes Can’t Tell. *PLOS ONE, 10*(3), e0119445. <https://doi.org/10.1371/journal.pone.0119445>

586 Cole, J. C. (2008). *How to deal with missing data: Conceptual overview and details for implementing*
587 *two modern methods*. In J. W. Osbourne (Ed.), *Best practices in quantitative methods* (pp.
588 214–238). Thousand Oaks: Sage Publications.

589 Da Costa, L., Parr, T., Sajid, N., Veselic, S., Neacsu, V., & Friston, K. (2020). Active inference on
590 discrete state-spaces: A synthesis. *ArXiv:2001.07203 [q-Bio]*.
591 <http://arxiv.org/abs/2001.07203>

592 Dayan, P., & Yu, A. J. (2003). Uncertainty and Learning. *IETE Journal of Research*, *49*(2–3), 171–181.
593 <https://doi.org/10.1080/03772063.2003.11416335>

594 de Brouwer, A. J., Flanagan, J. R., & Spering, M. (2021). Functional Use of Eye Movements for an
595 Acting System. *Trends in Cognitive Sciences*. <https://doi.org/10.1016/j.tics.2020.12.006>

596 Diaz, G., Cooper, J., & Hayhoe, M. (2013). Memory and prediction in natural gaze control.
597 *Philosophical Transactions of the Royal Society B: Biological Sciences*, *368*(1628), 20130064.
598 <https://doi.org/10.1098/rstb.2013.0064>

599 Diaz, G., Cooper, J., Rothkopf, C., & Hayhoe, M. (2013). Saccades to future ball location reveal
600 memory-based prediction in a virtual-reality interception task. *Journal of Vision*, *13*(1), 20–
601 20. <https://doi.org/10.1167/13.1.20>

602 Domínguez-Zamora, F. J., Gunn, S. M., & Marigold, D. S. (2018). Adaptive Gaze Strategies to Reduce
603 Environmental Uncertainty During a Sequential Visuomotor Behaviour. *Scientific Reports*,
604 *8*(1), 14112. <https://doi.org/10.1038/s41598-018-32504-0>

605 Fooker, J., & Spering, M. (2020). Eye movements as a readout of sensorimotor decision processes.
606 *Journal of Neurophysiology*, *123*(4), 1439–1447. <https://doi.org/10.1152/jn.00622.2019>

607 Friston, K. (2005). A theory of cortical responses. *Philosophical Transactions of the Royal Society B:*
608 *Biological Sciences*, *360*(1456), 815–836. <https://doi.org/10.1098/rstb.2005.1622>

609 Friston, K. (2010). The free-energy principle: A unified brain theory? *Nature Reviews Neuroscience*,
610 *11*(2), 127–138. <https://doi.org/10.1038/nrn2787>

611 Friston, K., Adams, R., Perrinet, L., & Breakspear, M. (2012). Perceptions as Hypotheses: Saccades as
612 Experiments. *Frontiers in Psychology, 3*. <https://doi.org/10.3389/fpsyg.2012.00151>

613 Friston, K., FitzGerald, T., Rigoli, F., Schwartenbeck, P., O'Doherty, J., & Pezzulo, G. (2016). Active
614 inference and learning. *Neuroscience & Biobehavioral Reviews, 68*, 862–879.
615 <https://doi.org/10.1016/j.neubiorev.2016.06.022>

616 Friston, K. J., Parr, T., & de Vries, B. (2017). The graphical brain: Belief propagation and active
617 inference. *Network Neuroscience, 1*(4), 381–414. https://doi.org/10.1162/NETN_a_00018

618 Friston, K., Kilner, J., & Harrison, L. (2006). A free energy principle for the brain. *Journal of*
619 *Physiology-Paris, 100*(1), 70–87. <https://doi.org/10.1016/j.jphysparis.2006.10.001>

620 Friston, K., Mattout, J., Trujillo-Barreto, N., Ashburner, J., & Penny, W. (2007). Variational free energy
621 and the Laplace approximation. *NeuroImage, 34*(1), 220–234.
622 <https://doi.org/10.1016/j.neuroimage.2006.08.035>

623 Glass, G. V. (1966). Note on Rank Biserical Correlation. *Educational and Psychological Measurement,*
624 *26*(3), 623–631. <https://doi.org/10.1177/001316446602600307>

625 Gray, R. (2020). Changes in Movement Coordination Associated With Skill Acquisition in Baseball
626 Batting: Freezing/Freeing Degrees of Freedom and Functional Variability. *Frontiers in*
627 *Psychology, 11*. <https://doi.org/10.3389/fpsyg.2020.01295>

628 Gray, R., & Cañal-Bruland, R. (2018). Integrating visual trajectory and probabilistic information in
629 baseball batting. *Psychology of Sport and Exercise, 36*, 123–131.
630 <https://doi.org/10.1016/j.psychsport.2018.02.009>

631 Gredin, N. V., Bishop, D. T., Broadbent, D. P., Tucker, A., & Williams, A. M. (2018). Experts integrate
632 explicit contextual priors and environmental information to improve anticipation efficiency.
633 *Journal of Experimental Psychology: Applied, 24*(4), 509–520.
634 <https://doi.org/10.1037/xap0000174>

635 Gredin, N. V., Bishop, D. T., Williams, A. M., & Broadbent, D. P. (2020). The use of contextual priors
636 and kinematic information during anticipation in sport: Toward a Bayesian integration

637 framework. *International Review of Sport and Exercise Psychology*, 0(0), 1–25.
638 <https://doi.org/10.1080/1750984X.2020.1855667>

639 Harris, D., Arthur, T., Broadbent, D., Wilson, M., Vine, S., & Runswick, O. (2021). *An active inference*
640 *account of skilled anticipation in sport*. PsyArXiv. <https://doi.org/10.31234/osf.io/2x3kg>

641 Hayhoe, M. M., McKinney, T., Chajka, K., & Pelz, J. B. (2012). Predictive eye movements in natural
642 vision. *Experimental Brain Research*, 217(1), 125–136. [https://doi.org/10.1007/s00221-011-](https://doi.org/10.1007/s00221-011-2979-2)
643 2979-2

644 Heilbron, M., & Meyniel, F. (2019). Confidence resets reveal hierarchical adaptive learning in
645 humans. *PLOS Computational Biology*, 15(4), e1006972.
646 <https://doi.org/10.1371/journal.pcbi.1006972>

647 Hein, T. P., de Fockert, J., & Ruiz, M. H. (2021). State anxiety biases estimates of uncertainty and
648 impairs reward learning in volatile environments. *NeuroImage*, 224, 117424.
649 <https://doi.org/10.1016/j.neuroimage.2020.117424>

650 Heinen, S. J., Badler, J. B., & Ting, W. (2005). Timing and velocity randomization similarly affect
651 anticipatory pursuit. *Journal of Vision*, 5(6), 1–1. <https://doi.org/10.1167/5.6.1>

652 Henderson, J. M. (2017). Gaze control as prediction. *Trends in Cognitive Sciences*, 21(1), 15–23.
653 <https://doi.org/10.1016/j.tics.2016.11.003>

654 Itti, L., & Baldi, P. (2009). Bayesian surprise attracts human attention. *Vision Research*, 49(10), 1295–
655 1306. <https://doi.org/10.1016/j.visres.2008.09.007>

656 Itti, L., & Koch, C. (2001). Computational modelling of visual attention. *Nature Reviews Neuroscience*,
657 2(3), 194–203. <https://doi.org/10.1038/35058500>

658 JASP team. (2018). *JASP (version 0.9)[computer software]*. Amsterdam, NLD: University of
659 Amsterdam.

660 Knill, D. C., & Pouget, A. (2004). The Bayesian brain: The role of uncertainty in neural coding and
661 computation. *Trends in Neurosciences*, 27(12), 712–719.
662 <https://doi.org/10.1016/j.tins.2004.10.007>

663 Körding, K. (2007). Decision Theory: What 'Should' the Nervous System Do? *Science*, 318(5850), 606–
664 610. <https://doi.org/10.1126/science.1142998>

665 Körding, K. P., & Wolpert, D. M. (2004). Bayesian integration in sensorimotor learning. *Nature*,
666 427(6971), 244–247. <https://doi.org/10.1038/nature02169>

667 Krassanakis, V., Filippakopoulou, V., & Nakos, B. (2014). EyeMMV toolbox: An eye movement post-
668 analysis tool based on a two-step spatial dispersion threshold for fixation identification.
669 *Journal of Eye Movement Research*, 7(1). <https://doi.org/10.16910/jemr.7.1.1>

670 Land, M. F. (2009). Vision, eye movements, and natural behavior. *Visual Neuroscience*, 26(1), 51–62.
671 <https://doi.org/10.1017/S0952523808080899>

672 Land, M. F., & McLeod, P. (2000). From eye movements to actions: How batsmen hit the ball. *Nature*
673 *Neuroscience*, 3(12), 1340–1345. <https://doi.org/10.1038/81887>

674 Lawson, R. P., Bisby, J., Nord, C. L., Burgess, N., & Rees, G. (2021). The Computational,
675 Pharmacological, and Physiological Determinants of Sensory Learning under Uncertainty.
676 *Current Biology*, 31(1), 163-172.e4. <https://doi.org/10.1016/j.cub.2020.10.043>

677 Loffing, F., & Cañal-Bruland, R. (2017). Anticipation in sport. *Current Opinion in Psychology*, 16, 6–11.
678 <https://doi.org/10.1016/j.copsyc.2017.03.008>

679 Mann, D. L., Nakamoto, H., Logt, N., Sikkink, L., & Brenner, E. (2019). Predictive eye movements
680 when hitting a bouncing ball. *Journal of Vision*, 19(14), 28–28.
681 <https://doi.org/10.1167/19.14.28>

682 Mann, D., Spratford, W., & Abernethy, B. (2013). The Head Tracks and Gaze Predicts: How the
683 World's Best Batters Hit a Ball. *PLOS ONE*, 8(3), e58289.
684 <https://doi.org/10.1371/journal.pone.0058289>

685 Mathys, C. D., Lomakina, E. I., Daunizeau, J., Iglesias, S., Brodersen, K. H., Friston, K. J., & Stephan, K.
686 E. (2014). Uncertainty in perception and the Hierarchical Gaussian Filter. *Frontiers in Human*
687 *Neuroscience*, 8, 825.

688 Meyniel, F., Maheu, M., & Dehaene, S. (2016). Human Inferences about Sequences: A Minimal
689 Transition Probability Model. *PLOS Computational Biology*, *12*(12), e1005260.
690 <https://doi.org/10.1371/journal.pcbi.1005260>

691 Meyniel, F., Schlunegger, D., & Dehaene, S. (2015). The sense of confidence during probabilistic
692 learning: A normative account. *PLOS Computational Biology*, *11*(6), e1004305.

693 Moritz, S., & Bartz-Beielstein, T. (2017). ImputeTS: Time Series Missing Value Imputation in R. *The R*
694 *Journal*, *9*(1), 207.

695 Mrotek, L. A., & Soechting, J. F. (2007). Target Interception: Hand–Eye Coordination and Strategies.
696 *Journal of Neuroscience*, *27*(27), 7297–7309. [https://doi.org/10.1523/JNEUROSCI.2046-](https://doi.org/10.1523/JNEUROSCI.2046-07.2007)
697 [07.2007](https://doi.org/10.1523/JNEUROSCI.2046-07.2007)

698 Najemnik, J., & Geisler, W. S. (2005). Optimal eye movement strategies in visual search. *Nature*,
699 *434*(7031), 387–391. <https://doi.org/10.1038/nature03390>

700 Nijhawan, R. (2008). Visual prediction: Psychophysics and neurophysiology of compensation for time
701 delays. *Behavioral and Brain Sciences*, *31*(2), 179–198.
702 <https://doi.org/10.1017/S0140525X08003804>

703 O’Sullivan, I., Burdet, E., & Diedrichsen, J. (2009). Dissociating Variability and Effort as Determinants
704 of Coordination. *PLOS Computational Biology*, *5*(4), e1000345.
705 <https://doi.org/10.1371/journal.pcbi.1000345>

706 Parr, T., & Friston, K. J. (2019). Generalised free energy and active inference. *Biological Cybernetics*,
707 *113*(5), 495–513. <https://doi.org/10.1007/s00422-019-00805-w>

708 Rao, R. P. N., & Ballard, D. H. (1999). Predictive coding in the visual cortex: A functional
709 interpretation of some extra-classical receptive-field effects. *Nature Neuroscience*, *2*(1), 79–
710 87. <https://doi.org/10.1038/4580>

711 Rauss, K., & Pourtois, G. (2013). What is Bottom-Up and What is Top-Down in Predictive Coding?
712 *Frontiers in Psychology*, *4*. <https://doi.org/10.3389/fpsyg.2013.00276>

713 Reid, M., Elliott, B., & Crespo, M. (2013). Mechanics and Learning Practices Associated with the
714 Tennis Forehand: A Review. *Journal of Sports Science & Medicine*, *12*(2), 225–231.

715 Rigoux, L., Stephan, K. E., Friston, K. J., & Daunizeau, J. (2014). Bayesian model selection for group
716 studies—Revisited. *NeuroImage*, *84*, 971–985.
717 <https://doi.org/10.1016/j.neuroimage.2013.08.065>

718 Runswick, O. R., Roca, A., Williams, A. M., & North, J. S. (2020). A Model of Information Use During
719 Anticipation in Striking Sports (MIDASS). *Journal of Expertise*, *3*(4), 197–211.

720 Shipp, S., Adams, R. A., & Friston, K. J. (2013). Reflections on agranular architecture: Predictive
721 coding in the motor cortex. *Trends in Neurosciences*, *36*(12), 706–716.
722 <https://doi.org/10.1016/j.tins.2013.09.004>

723 Smith, R., Friston, K., & Whyte, C. (2021). *A Step-by-Step Tutorial on Active Inference and its*
724 *Application to Empirical Data*. PsyArXiv. <https://doi.org/10.31234/osf.io/b4jm6>

725 Smith, R., Kuplicki, R., Feinstein, J., Forthman, K. L., Stewart, J. L., Paulus, M. P., Investigators, T.
726 1000, & Khalsa, S. S. (2020). A Bayesian computational model reveals a failure to adapt
727 interoceptive precision estimates across depression, anxiety, eating, and substance use
728 disorders. *PLOS Computational Biology*, *16*(12), e1008484.
729 <https://doi.org/10.1371/journal.pcbi.1008484>

730 Stevenson, I. H., Fernandes, H. L., Vilares, I., Wei, K., & Körding, K. P. (2009). Bayesian Integration
731 and Non-Linear Feedback Control in a Full-Body Motor Task. *PLOS Computational Biology*,
732 *5*(12), e1000629. <https://doi.org/10.1371/journal.pcbi.1000629>

733 van Doorn, J., van den Bergh, D., Bohm, U., Dablander, F., Derks, K., Draws, T., Evans, N. J., Gronau,
734 Q. F., Hinne, M., Kucharský, Š., Ly, A., Marsman, M., Matzke, D., Raj, A., Sarafoglou, A.,
735 Stefan, A., Voelkel, J. G., & Wagenmakers, E.-J. (2019). *The JASP Guidelines for Conducting*
736 *and Reporting a Bayesian Analysis* [Preprint]. PsyArXiv.
737 <https://doi.org/10.31234/osf.io/yqxfr>

738 Wyart, V., & Koechlin, E. (2016). Choice variability and suboptimality in uncertain environments.
739 *Current Opinion in Behavioral Sciences*, *11*, 109–115.
740 <https://doi.org/10.1016/j.cobeha.2016.07.003>

741 Yu, A. J., & Dayan, P. (2005). Uncertainty, Neuromodulation, and Attention. *Neuron*, *46*(4), 681–692.
742 <https://doi.org/10.1016/j.neuron.2005.04.026>

743 Zago, M., Bosco, G., Maffei, V., Iosa, M., Ivanenko, Y. P., & Lacquaniti, F. (2004). Internal models of
744 target motion: Expected dynamics overrides measured kinematics in timing manual
745 interceptions. *Journal of Neurophysiology*, *91*(4), 1620–1634.
746 <https://doi.org/10.1152/jn.00862.2003>

747 Zhao, H., & Warren, W. H. (2015). On-line and model-based approaches to the visual control of
748 action. *Vision Research*, *110*, 190–202. <https://doi.org/10.1016/j.visres.2014.10.008>
749

750

Supplementary Materials

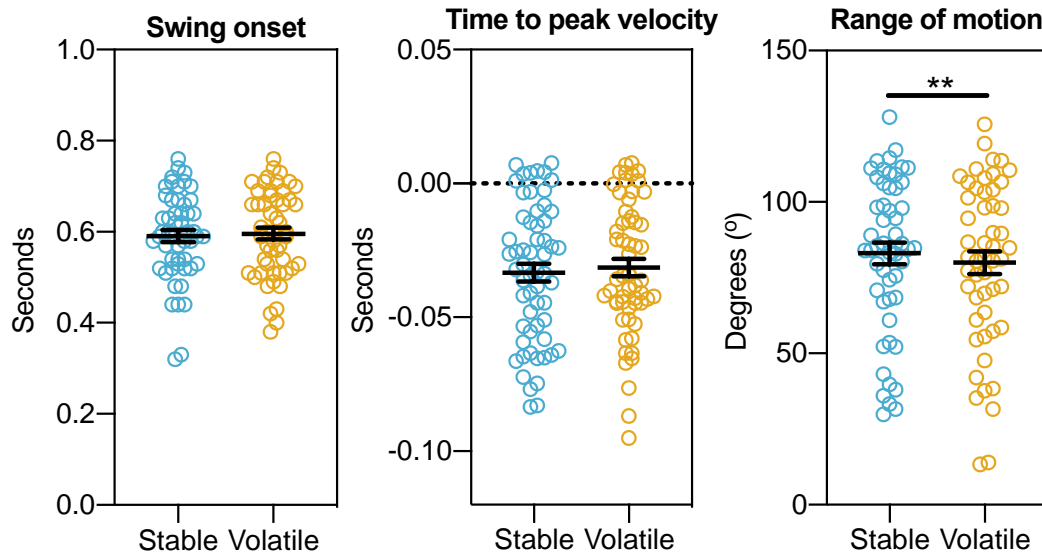
751 **Motor Kinematics Analysis**

752 In our main analyses, we observed that participants' gaze responses were adjusted in a
753 Bayes-optimal fashion. Yet, active inference mechanisms not only relate to how an individual
754 samples the world, they are also said to underpin how an agent acts upon their surrounding
755 environment (e.g., through motor initiation, movement adjustments). Accordingly, we extracted
756 several additional swing kinematic variables from our interceptive racquetball data (collected in the
757 context of examining sensorimotor control in Autism, available at: <https://osf.io/ewnh9/>), to
758 illustrate whether participants' motor responses were consistent with Bayes-optimal control.

759 As decision times are modulated according to uncertainty (Lawson et al., 2021), swing onset
760 (the first frame in which forward motion of the racket began) and time to peak swing velocity (the
761 square root of the sum of squared vector differentials) were calculated during the fore swing phase
762 of movement. Here, attenuations in the use of prior knowledge might be reflected in later
763 movement onsets and/or disrupted velocity profiles. Furthermore, swing range of motion (ROM; °)
764 was calculated from the angular deviation of the hand controller in the transverse plane during the
765 foreswing. Reductions in swing ROM values indicate greater 'fixing' or 'freezing' of movement
766 degrees of freedom that are associated with poorer motor control (Bernstein, 1967; Gray, 2020).
767 Under uncertain conditions joint stiffness can be increased and multi-effector redundancy can be
768 restricted to reduce uncertainty (i.e., from signal-dependent noise; O'Sullivan et al., 2009)).
769 Consequently, we hypothesised that ROM would be sensitive to changes in environmental stability,
770 and that performers would show restricted degrees of freedom under more volatile conditions.

771 Paired t-tests indicated no differences between stable and volatile conditions, for either
772 swing onset times ($t(51) = 0.86$, $p = .39$, $d = 0.12$, $BF_{10} = 0.22$) or time of peak swing velocity ($t(51) =$
773 0.18 , $p = .86$, $d = 0.02$, $BF_{10} = 0.15$). This suggests that the volatile context did not delay the motor
774 action or disrupt hand velocity profiles over time. There were, however, differences in ROM
775 (Supplementary Fig 1). Specifically, paired t-tests indicated a significantly reduced ROM in the
776 volatile ($M = 79.9$, $SD = 27.2$) compared to the stable condition ($M = 83.1$, $SD = 25.6$; $t(51) = 2.74$, $p =$
777 $.008$, $d = 0.38$), with moderate Bayesian support for our alternative hypotheses ($BF_{10} = 4.32$). These
778 motor patterns are indicative of more novice-like swing kinematics (Bernstein, 1967; Reid et al.,
779 2013), highlighting that a regression towards simpler movement patterns (i.e., 'fixing' of joint angles)
780 may serve as an active attempt for minimising movement uncertainty (O'Sullivan et al., 2009).

781 Overall, these results support our main observations, that not only did people adjust their
782 expectations about likely ball trajectories in a Bayes-optimal fashion, but that those predictions
783 influenced gaze behaviours *and* motor responses.



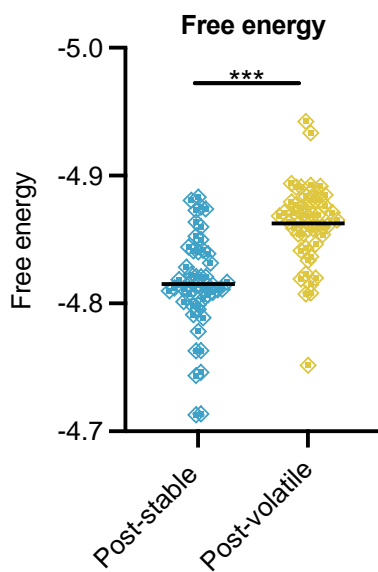
784
785 **Supplementary Fig 1. Movement variables.** Dot plots (with mean and standard error) comparing
786 kinematic variables between stable and volatile conditions. Note: * $p < .05$, ** $p < .01$.

787
788 **Simulations of model free energy during order-matched trials**

789 Within an active inference framework, the optimal learning strategy when faced with
790 environmental volatility is to track not only trial-to-trial probabilities but also wider shifts in
791 probabilistic relationships (Meyniel et al., 2015). These dynamic computations generally assume a
792 hierarchical generative model of the world, whereby higher-level beliefs about hidden
793 environmental states modulate lower-level prediction errors (Behrens et al., 2007). However,
794 previous work has found that single-level models, or flat approximations of hierarchical models, can
795 better explain learning in some instances (Bell et al., 2016; Heilbron & Meyniel, 2019; Wyart &
796 Koechlin, 2016). Although a ‘flat’ model could potentially account for changes in learning rate during
797 volatile trial periods (e.g., due to down-weighting of predictions relative to sensory information
798 when trial to trial contingencies are more uncertain), single-level explanations cannot easily explain
799 why learning rate varies when there is an *awareness* of change (Heilbron & Meyniel, 2019).
800 Consequently, the increase in learning rate for the post-stable trials in our data is generally
801 suggestive of hierarchical rather than single-level learning.

802 While our design did not allow us to fully disambiguate hierarchical and flat model origins of
803 learning rate (but see Heilbron & Meyniel, 2019), we ran additional simulations using the POMDP

804 model in Fig. 2 to determine what effect our hierarchical model would predict for the order matched
 805 trials that followed stable or volatile periods. This supplementary analysis specifically focused on the
 806 size of prediction errors (VFE) in the post-stable and post-volatile order-matched trials. By studying
 807 these parameters after a *change point* in our ball bounciness trial sequences, we could understand
 808 how volatility computations affect prediction error (and learning rate) in this particular hierarchical
 809 system. Simulations showed that prediction error was markedly influenced by the preceding
 810 environmental volatility, with VFE profiles clearly contrasting between post-stable and post-volatile
 811 blocks (see Supplementary Fig 2).



812
 813 **Supplementary Fig 2.** Dot plots (with mean) of model VFE for the 9 order-matched trials following
 814 periods of stable and volatile trial sequences. *** $p < .001$

815 Interestingly, and in contrast to our behavioural data, these simulations indicated higher
 816 prediction errors for the *post-volatile* ($M = -4.86$, $SD = 0.04$), as opposed to *post-stable* ($M = -4.82$,
 817 $SD = 0.03$), trials ($t(49) = 7.55$, $p < .001$, $d = 1.07$) (see Supplementary Fig 2). The reason for this is that the
 818 higher level of our model encoded beliefs about stability/volatility, meaning that agents were
 819 encoding the wider unpredictability of their environment in the subsequent order-matched trials.
 820 Our behavioural observations of higher learning rates in post-stable conditions (Fig.5) may indicate
 821 that participants were actually more sensitive to the abrupt change that followed a period of
 822 stability, compared to the persistent changeability of the volatile condition. While often used
 823 interchangeably, Bland and Schaefer (2012) distinguish between the concepts of volatility and
 824 unexpected uncertainty, where unexpected uncertainty refers to rare unpredicted environmental
 825 shifts whereas high volatility is a more frequent fundamental change. Similarly, Mathys et al. (2014)
 826 outline how multi-level representations of volatility in the Hierarchical Gaussian Filter model are

827 themselves controlled by volatility parameters, such that the volatility of the environment can be
828 more or less changeable (and so on). The implication of these descriptions is that unpredictable
829 shifts can almost come to be expected. Our behavioural results might, then, be explained by
830 participants' beliefs that the volatile condition was highly unpredictable, and would continue to be
831 so, whereas the shift after the post-stable condition was less expected and worth adapting to.
832 However, this kind of expectation about the persistence of the volatility was not captured in our
833 hierarchical model. As such, it must be stressed that these interpretations remain speculative at this
834 stage and further work should seek to decipher how higher-level expectations of volatility are
835 encoded.